The Beneficial and Detrimental Effects of Rocking Shallow Foundations on Super Structure during Seismic Loading

Partheeban Selvarajah[1] & Sivapalan Gajan[2]
[1]Ph.D. Student and [2]Associate Professor, Department of Civil & Environmental Engineering – North Dakota State University, Fargo, North Dakota, USA

ABSTRACT
Generally, modern seismic design codes prohibit relative movement between the foundation and the soil beneath, which demands the structural elements of the superstructure to dissipate seismic energy. The primary benefit of appropriately reducing the size of the footing in shallow foundation is the partial isolation of the structure from the soil beneath (uplift and rocking). The rocking behavior caused by the seismic loading can occur around the footing base, subsequently dissipating the seismic energy and reducing the ductility demands transmitted to the superstructure. In this study, several centrifuge and shake table experiments on rocking shallow foundations have been analyzed to investigate the following beneficial and detrimental effects in an attempt to come up with a balanced design methodology: reliability and predictability of the moment capacity of the soil-foundation system, rocking induced energy dissipation and the resulting permanent settlement of the foundation, and the reduced ductility demands (maximum and permanent tilt of the structure) transmitted to the super structure.

RÉSUMÉ
Généralement, les codes de conception sismiques modernes interdisent le mouvement relatif entre la fondation et le sol en dessous de celle-ci, ce qui exige que les éléments structurels de la superstructure dissipent l'énergie sismique. Le principal avantage, de réduire de manière appropriée la taille de la semelle en fondation superficielle, est l'isolement partiel de la structure du sol en dessous (soulèvement et basculement). Le comportement basculant causé par la charge sismique peut se produire autour de la base de pied, ce qui permet la dissipation de l'énergie sismique, réduisant ainsi les exigences de ductilité transmises à la superstructure. Cette étude comprend plusieurs expériences sur des fondations superificielles basculantes avec des centrifugeuses et des tables vibrantes. Les résultats ont été analysés pour enquêter sur la fiabilité et la prévisibilité de la capacité du moment du système sol-fondation, le tassement permanent induit par le basculement, la méthodologie de conception d'équilibrage utilisant le tassement total et le coefficient de basculement pour fondation basculante (pour obtenir des valeurs optimales pour les paramètres de conception), et la réduction des exigences de ductilité transmises à la superstructure (en raison de la dissipation d'énergie sismique induite par le basculement).

1 INTRODUCTION

Earthquakes are one of the most devastating types of natural disasters occurring around the world. One recent example is the Nepal earthquake on April 25, 2015 with a magnitude of 7.8. It is daunting to imagine that a single, magnitude 7 earthquake in New York in the United States could result in up to $200 Billion in direct and indirect losses (Tantala et al., 2008). In general, in seismic zones, the majority of the damage occurs at the base of the columns (Arslan et al., 2007) which leads to complete destruction of structures. The modern design codes prohibits relative movement between the foundation and underlying soil. In this conventional design of shallow foundation approach according to capacity principles, it is generally recognized that any damage to the foundation should be avoided, while the nonlinear behavior of structural components are used to improve the performance of buildings (Pitilakis et al., 2007). This contradicts modern research interest towards performance based approaches for seismic design. Performance based design philosophy should consider all sources of nonlinearities developed above the ground in structural elements and below ground level in foundation soil (Zafeirakos et al., 2014).

To date, there are a growing number of experimental studies, which illustrated that foundation rocking can be advantageously used to dissipate part of the seismic energy into the foundation soil which also provides self-centering of the structural system (Paolucci et al., 2008, Gajan and Kutter, 2008 and 2009, Anastasopoulos et al., 2010 and 2013, Deng et al., 2012, Drosos et al, 2012, Ugalde et al., 2007). Over the past few years significant advancements have been made on understanding rocking shallow foundations' response to earthquake loading.

This paper discusses the alternative foundation design to conventional shallow foundation design in seismically active areas to prevent structural damage by taking the advantage of nonlinearity of the soil below foundations. This paper summarises experimental finding on rocking shallow foundation conducted all over the world. Specifically, this paper addresses the reliability of the moment capacity of the rocking foundation, rocking induced seismic energy dissipation, resulting settlement of foundation, and rocking induced maximum and residual tilt of the structure.

2 PROBLEM DEFINITATION

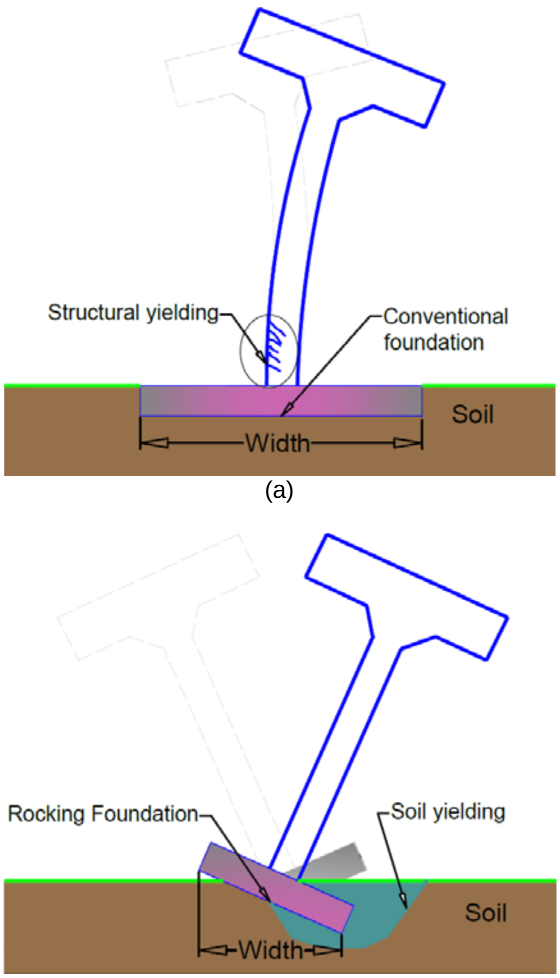

Figure 1. Illustrations of the concept of conventional foundation design (a) with rocking foundation design (b).

In conventional shallow foundation design, footings are intentionally designed so large that the plastic hinging would occur at the column base during seismic loading. In the proposed rocking foundation designed, footings can be designed by appropriately reducing their size so that the nonlinear behavior of soil can be utilized (plastic hinging at soil-foundation interface). The primary reason for conventional designed philosophy is that if damage occurs above ground, it can be retrofitted relatively easier. However, a growing body of knowledge now suggest that by forcing the plastic hinging into foundation soil, several advantageous features could be utilized.

2.1 Rocking Shallow Foundation

Housner (1963) observed golf-ball-on-a-tee types of elevated water tanks survived during the Chilean earthquake of May 1960 while more modern structures were severely damaged. Figure 2 schematically illustrates a simplified SDOF relatively rigid structure-footing model supported by relatively flexible soil. Also shown in Figure 2 are the key forces and displacements experienced by the soil-foundation-structure model during seismic loading (note that the moment induced by the lateral seismic inertia force (F) causes uplift and rocking at soil-foundation interface).

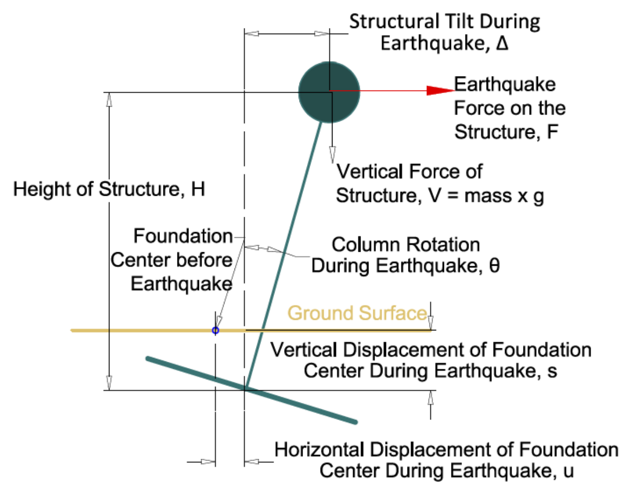

Figure 2. Idealized rigid (SDOF) structure-foundation system supported by nonlinear soil.

Rocking shallow foundations have many features that are yet to be implemented in earthquake engineering practice in protecting the structures and reducing the construction cost. The shearing of soil beneath the foundation will dissipate energy through friction, and, due to uplift associated with rocking, shallow foundations possess significant self centering characteristics (Gajan and Kutter, 2008). However, the concerns about permanent deformations below foundation and the concerns about total tipping-over failure have hindered the use of rocking foundations in practice.

2.2 Objectives of the Paper

The objective of this paper is to quantify some of the beneficial and detrimental effects of rocking shallow foundations based on experimental research. These parameters include reliability and predictability of the moment capacity of the soil-foundation system, rocking induced energy dissipation and the resulting permanent settlement of the foundation, and the reduced ductility demands (maximum and permanent tilt of the structure) transmitted to the super structure.

3 THEORY AND DEFINITION OF PARAMETERS

Deng et al. (2012) showed that plastic hinging can be forced to occur at foundation soil during rocking by making sure that the rocking coefficient (C_r) is smaller than the base shear coefficient (C_y) of the column; where C_r and C_y are non-dimensional moment capacities of soil-foundation system and column respectively.

The rocking coefficient depends on two parameters: critical contact area ratio of the soil-foundation system (A/A_c) and the aspect ratio of the structure (H/B); where A is the total base area of the footing, A_c is the minimum footing contact area required to support the applied vertical loads on the foundation (which can be calculated from conventional bearing capacity equation (static) and the associated shape and depth factors) (Gajan and Kutter, 2008), H is the effective height of the structure (Fig. 2) and B is the width of the footing in the direction of shaking (Fig. 1). By considering equilibrium equations and the moment capacity of soil-foundation system, the following equation can be derived for C_r:

$$C_r = \frac{B}{2 \times H}\left(1 - \frac{A_c}{A}\right) \quad [1]$$

The base shear coefficient (C_y) for a reinforced concrete (RC) column is defined as the ratio of moment capacity of column (M_{cap_col}) to the weight (V) of the structure normalized by the effective height (H):.

$$C_y = \frac{M_{cap\_col}}{V \times H} \quad [2]$$

One way of quantifying the intensity of the earthquake is Arias intensity (Kramer, 1996). Arias intensity (I_a) combines the magnitude, frequency content, and duration of the earthquake and is defined as,

$$I_a = \frac{\pi}{2g}\int_0^{\infty} [a(t)]^2\, dt \quad [3]$$

Where g is the gravitational acceleration and a(t) is the acceleration time history of the earthquake in time domain (t).

The rocking induced total settlement is primarily a function of two key parameters, C_r and I_a, as they incorporate the effects of foundation geometry, aspect ratio of the structure, soil parameters, and intensity of the earthquake:

$$S_{Total} = f(C_r, I_a) \quad [4]$$

It was hypothesized that the amount of energy dissipation (ED) at the foundation soil is primarily a function of two key parameters discussed earlier, C_r and S_{Total}.

$$ED = f(C_r, S_{Total}) \quad [5]$$

It was found that the rocking induced maximum rotation (θ_{max}) of the foundation, on the other hand, is primarily a function of aspect ratio of the structure (H/B) and maximum acceleration of the earthquake (a_{max}).

$$\theta_{max} = f\left(\frac{H}{B}, a_{max}\right) \quad [6]$$

For relatively rigid structures supported by rocking foundations, the maximum lateral displacement at the height of center of gravity of the structure (Δ_{max}) can then obtained by,

$$\Delta_{max} = \theta_{max} \times H \quad [7]$$

Permanent tilt (Δ_{per}) of the foundation is one of the important parameter that needs to be investigated at the end of the earthquake to determine the severity of the damage. It is a function of maximum acceleration of the earthquake (a_{max}) and θ_{max}:

$$\Delta_{per} = f(a_{max}, \theta_{max}) \quad [8]$$

For relatively rigid structures supported by rocking foundations, the permanent lateral displacement at the height of center of gravity of the structure (Δ_{per}) can then obtained by multiplying the permanent rotation of the structure at the end of the earthquake (θ_{per}) by effective height of the structure(H).

$$\Delta_{per} = \theta_{per} \times H \quad [9]$$

The amount of energy dissipation (ED) in foundation soil during rocking comes primarily from the area of the hysteresis loops in the cyclic moment-rotation (M-θ) relation of the soil-foundation system,

$$ED = \int_0^{\theta_{fin}} M\, d\theta \quad [10]$$

A non-dimensional energy dissipation (NED) was then obtained by normalizing ED by the weight of the structure (V) and the dimension of the footing in the direction of shaking (B),

$$NED = \frac{ED}{V.B} \quad [11]$$

4 EXPERIMENTAL PROGRAMS

Results of seventeen centrifuge experiments conducted at University of California, Davis (UCD) (Ugalde et al., 2007 and Gajan and Kutter, 2008) and the results of fifteen shaking table experiments conducted at the National Technical University of Athens (NTUA), Greece (Drosos et al., 2012, and Anastasopoulos et al., 2013) have been considered in this study.

4.1 Types of soils, foundations, structures and loading

The soil type used in UCD experiments was dry Nevada sand (D_r = 80% and Φ = 42^o) while the soil type used in NTUA experiments was dry Quartz sand (D_r = 85% and Φ = 44^o). The properties of both sands are similar, which makes the comparisons meaningful. Gajan and Kutter (2008) tested rigid shear wall structures supported by shallow foundations while Ugalde et al. (2007) modeled relatively flexible reinforced concrete columns connected to a bridge deck mass supported by shallow foundations. In NTUA experiments, deck mass connected to rigid columns supported by shallow foundations were used. Note that majority of the experiments were conducted on surface footings while some experiments included a shallow embedment of the footings in soil. Both UCD and NTUA experiments included base shaking of actual earthquake recordings and artificially generated acceleration time histories as well (e.g., sine waves). Table 1 lists the important data and parameters used in this study to analyze the results.

5 RESULTS AND DISCUSSION

5.1 Energy dissipation and permanent settlement of foundation soil

Figure 3 shows that the maximum rotation of the structure (θ_{max}) during the earthquake can be correlated with the maximum acceleration of the earthquake (a_{max}) for different clusters of aspect ratio of the structure (H/B). As expected, θ_{max} increases as a_{max} increases. Though the data show some scatter, in general, higher H/B structures rotate more than their lower counterparts indicating the ability of slender structures to rock more than shorter structures.

Rocking induced total permanent settlement (S_{Total}) was obtained from the cyclic settlement-rotation relationships presented in the literature. Figure 4 presents the variation of total normalized permanent settlement of the foundation (S_{Total}/B) with maximum rotation (θ_{max}) of the structure. The results are grouped based on the Arias intensity (I_a) of the earthquake: for I_a value greater than 2.4 m/s and less than 2.4 m/s. As expected, as the rocking amplitude of the structure increases, the permanent settlement increases. There is a clear trend of separation in the results according to the I_a values, which in general indicate that I_a value less than 2.4 m/s earthquakes produce S_{Total}/B and θ_{max} that are less than 0.01. Both S_{Total}/B and θ_{max} increases as the intensity of the earthquake (I_a) increases. Overall, given I_a and B, normalized permanent settlement and θ_{max} can be correlated with reasonable accuracy. Note that a 1:1 line is also included in Figure 4 just to show the beneficial effect of normalizing the parameters and making them non-dimensional.

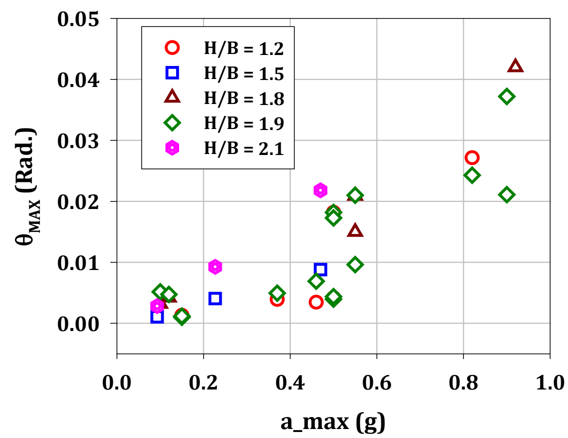

Figure 3 Variation of maximum rotation (θ_{max}) with a_{max} and H/B

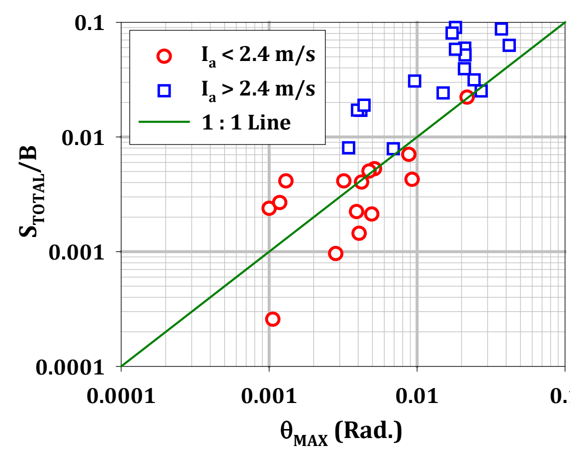

Figure 4 Variation of rocking induced permanent settlement with maximum rotation and Arias intensity (I_a)

Figure 5 presents the variation of (S_{Total}/B) with normalized energy dissipation in the foundation soil (ED/V.B) for two results groups of rocking coefficient (C_r): for C_r values greater than 0.25 and less than 0.25. Since plastic permanent settlement is a consequence of energy dissipation, the settlement increases as energy dissipation increases. There is a clear trend of higher normalized settlement for smaller C_r values. This is intuitive because as C_r decreases, the tendency of the footing rocking increases and hence more rocking induced settlement and energy dissipation. Overall, based on the thirty two experimental results, given B and C_r (parameters that do not depend on the earthquake), the total settlement of a rocking system can be correlated with ED/(V.B) with reasonable accuracy.

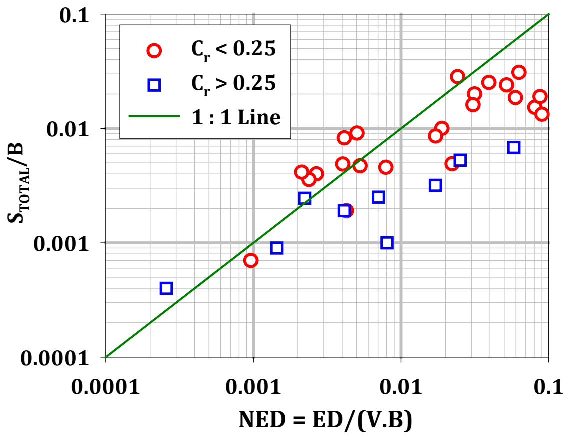

Figure 5 Relationship between rocking induced permanent settlement and energy dissipation with rocking coefficient (C_r)

In summary, by using Figures 3 through 5, the following parameters can be correlated: (1) Using a_{max} and H/B ratio, the earthquake induced maximum rotation (θ_{max}) can be estimated, (2) Using (θ_{max}) and Arias intensity of the earthquake (I_a), normalized permanent settlement of the foundation (S_{Total}/B) can be estimated, and (3) Using (S_{Total}/B) and rocking coefficient (C_r), the normalized seismic energy dissipation in foundation soil (ED/(V.B)) can be estimated.

5.2 Maximum, permanent, and critical rotation of the foundation

Figure 6 presents the permanent rotation (θ_{per}) of the structure (at the end of the earthquake) as a function of the maximum rotation (θ_{max}) of the structure during the earthquake for two different groups of Arias intensity of the earthquake (I_a): for I_a values greater than 2.4 m/s and less than 2.4 m/s. As (θ_{max}) increases, so does (θ_{per}) of the structure and during higher intensity earthquakes, both (θ_{max}) and (θ_{per}) increase. All the data points presented in Figure 6 fall below the 1:1 line plotted in (θ_{per}) versus (θ_{max}) space. This indicates the self-centering ability of the rocking foundations. Though the structure experienced a higher maximum rotation during the earthquake, its permanent rotation at the end of the earthquake is smaller than its maximum. If the data points plot farther away from the 1:1 line, that indicates a higher self-centering ability of rocking foundation.

Critical rotation of the structure (θ_{crit}) is defined as the rotation that would cause tipping over failure of the structure during earthquake. The maximum horizontal displacement at the center of gravity of the structure during earthquake that would cause tipping over failure during the earthquake is (B–B_c)/2, where B is the width of the footing in the direction of shaking and B_c is the critical contact with of the footing with the soil that is required to support applied vertical loads (Deng et al., 2012). For rectangular and square footings, the A_c and A terms are proportional to B_c and B, respectively, where A/A_c is the critical contact area ratio defined in section 3. The (θ_{crit}) can then be defined as,

$$\theta_c = \tan^{-1}\left(\frac{B - B_c}{2H}\right) \qquad [12]$$

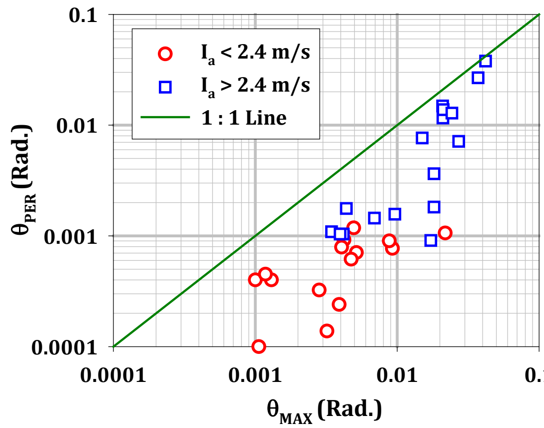

Figure 6 Variation of rocking induced permanent rotation with maximum rotation and Arias intensity (I_a)

Figure 7 presents the ratio of critical rotation to maximum rotation of the structure ($\theta_{crit}/\theta_{max}$) during the earthquake as a function of maximum acceleration (a_{max}) of the earthquake for different clusters of aspect ratio (H/B) of the structure. It should be noted that the ratio of ($\theta_{crit}/\theta_{max}$) can be considered as the stability (factor of safety) against tipping over failure of the structure during the earthquake. As can be seen from Figure 7, the higher tendency of rocking of taller structures produces smaller ratios of ($\theta_{crit}/\theta_{max}$) values and as expected the ratio of ($\theta_{crit}/\theta_{max}$) decreases as the intensity of the earthquake increases. However, the ratio of ($\theta_{crit}/\theta_{max}$) is as high as 200 for smaller magnitude earthquakes and 5 for high intensity earthquakes, indicating excellent stability against tipping over failure.

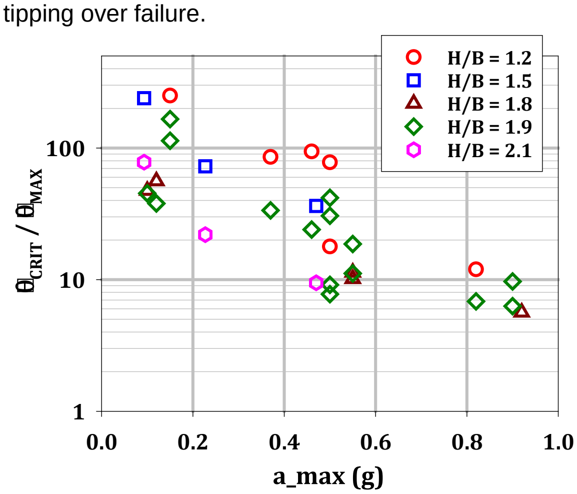

Figure 7 The variation of the ratio of critical (tip-over) rotation to maximum rotation with a_{max} and H/B

5.3 Ultimate moment capacity of rocking foundations

The theoretical ultimate moment capacity of a rocking foundation can be obtained using the following equation:

$$M_{ult} = \frac{VB}{2}\left[1 - \frac{A_c}{A}\right] \quad [13]$$

Where, V is the applied vertical load on the foundation, B is the width of the footing in the direction of shaking, and A_c/A is the inverse of critical contact area ratio of the foundation (Gajan and Kutter, 2008).

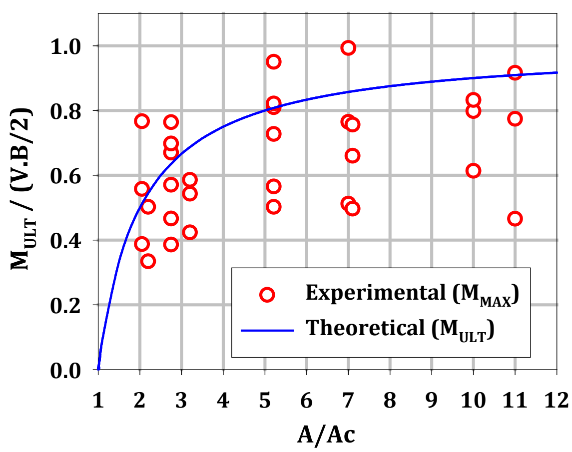

Figure 8 Comparison of theoretical ultimate moment capacity with experimentally measured maximum moment of soil-foundation interface.

Figure 8 presents the variation of normalized ultimate moment ($M_{ult}/(V.B/2)$) with A/Ac for both theoretical and experimental data. Experimental ultimate moment capacity values have been obtained as the maximum moment the foundation experienced during the earthquake. It should be noted that the theoretical normalized ultimate moment should vary within 0 and 1, as the minimum and maximum values of A_c/A is 0 and 1. As A/A_c increases, ($M_{ult}/(V.B/2)$) increases; however the experimental data points show significant scatter. During some of the earthquake shaking, the foundations were not loaded up to their ultimate moment capacity (small magnitude earthquakes). That explains why most of the data points fall below the theoretical failure envelope of ($M_{ult}/(V.B/2)$).

6 CONCLUSIONS

This paper summarized and analyzed thirty two centrifuge and shaking table experimental results of rocking shallow foundations. The results for rocking induced seismic energy dissipation and the corresponding total permanent settlement of the foundation, maximum rotation of the foundation during the earthquake and permanent rotation of the foundation at the end of the earthquake, and the ultimate moment capacity of the foundation and maximum moment experienced by the foundation are presented. These results are correlated with maximum acceleration and Arias intensity of the earthquake, aspect ratio of the structure, critical contact area ratio, and rocking coefficient of the foundation. The following conclusions are derived from the data presented in this paper:

1. Maximum rotation experienced by the structure/foundation during the earthquake can be correlated reasonably well with a_{max} and H/B. The permanent settlement of the foundation at the end of the earthquake can be correlated reasonably well with maximum rotation of the foundation and Arias intensity of the earthquake.
2. The results presented in this paper confirmed the hypothesis that rocking systems with small C_r values (compared to C_y values) have a higher tendency to rock and hence would result in higher seismic energy dissipation. However this higher energy dissipation comes at the expense of higher permanent settlement and higher maximum rotation.
3. The self-centering capacity of the rocking foundation can be quantified by comparing the permanent rotation of the foundation with the maximum rotation during the earthquake. The experimental results presented in this paper shows significant self-centering capacity of rocking foundations even during higher magnitude earthquakes.
4. The stability of the structure against tipping over failure during the earthquake can be quantified using the ratio of (θ_{crit}/ θ_{max}). Results show that the stability against tipping over failure is significantly higher than the common general perception. It should be noted that the concerns about tipping over failure have hindered the use of rocking foundations in civil engineering practice. In contrast, the factor of safety against tipping over failure of rocking foundations are well above 5 even for higher intensity earthquakes.

REFERENCES

Anastasopoulos, I., Gazetas, G., Loli, M., Apostolou, M., and Gerolymos, N. (2010). "Soil failure can be used for seismic protection of structures." *Bulletin of Earthquake Engineering*, 8(2), 309-326.

Anastasopoulos, I., Loli, M., Georgarakos, T., and Drosos, V. (2013). "Shaking Table Testing of Rocking-Isolated Bridge Pier on Sand." *Journal of Earthquake Engineering*, 17(1), 1-32.

Arslan, M. H., and Korkmaz, H. H. (2007). "What is to be learned from damage and failure of reinforced concrete structures during recent earthquakes in Turkey?" *Engineering Failure Analysis*, 14(1), 1-22.

Deng, L., Kutter, L. B., and Kunnath, K. S. (2012). "Centrifuge Modeling of Bridge Systems Designed for Rocking Foundations." *Journal of Geotechnical and Geoenvironmental Engineering*, 138(3), 335-344.

Drosos, V., Georgarakos, T., Loli, M., Anastsopoulos, I., Zarzouras, O., and Gazetas, G. (2012). "Soil-Foundation-Structure Interaction with Mobilization of Bearing Capacity: Experimental Study on Sand." *Journal of Geotechnical and Geoenvironmental Engineering*, 138(11), 1369–1386.

Gajan, S., and Kutter, B. L. (2008). "Capacity, Settlement, and Energy Dissipation of Shallow Footings Subjected to Rocking." *Journal of Geotechnical and Geoenvironmental Engineering*, 134(8), 1129-1141.

Housner, W. G. (1963). "The Behavior of Inverted Pendulum Structures during Earthquakes." *Bulletin of the Seismological Society of America.* 53(2), 403-417.

Paolucci, R., Shirato, M., and Yilmaz, M. T. (2008). "Seismic behaviour of shallow foundations: Shaking table experiments vs numerical modelling." *Earthquake Engineering & Structural Dynamics*, 37(4), 577-595.

Pitilakis, K., Gazetas, G., Anastasopoulos, I., and Apostolou, M. (2007). "Shallow and Deep Foundations under Fault Rupture or Strong Seismic Shaking." *Earthquake Geotechnical Engineering*, Springer Netherlands, 185-215.

Tantala, M. W., Nordenson, G. J. P., Deodatis, G., and Jacob, K. (2008). "Earthquake loss estimation for the New York City Metropolitan Region." *Soil Dynamics and Earthquake Engineering*, 28(10–11), 812-835.

Ugalde, A. J., Kutter, B. L., Jeremic, B., and Gajan, S. (2007). "Centrifuge Modeling of Rocking Behaviour of Bridges on Shallow Foundations." *4th International Conference on Earthquake Geotechnical Engineering*Thessaloniki, Greece.

Zafeirakos, A., and Gerolymos, N. (2014). "Towards a seismic capacity design of caisson foundations supporting bridge piers." *Soil Dynamics and Earthquake Engineering*, 67(0), 179-197.

APPENDIX

Table 1. Data for the settlement, rotation and energy dissipation graphs

#	C_r [1]	FS_v [2]	A/A_c [3]	B[4] (m)	a_{max} [5]	S_{Total} [6] (mm)	θ_{max} [7] ($radx10^{-3}$)	H[8] (m)	Δ_{max} [9] (mm)	Δ_{per} [10] (mm)	I_a [11] (m/s)	E_{dis} [12] (kN.m)	V[13] (kN)
1	0.13	2.3	2.1	7.0	0.2	28.0	1.2	13.3	15.7	6.0	1.192	251.69	13.4
2	0.13	2.3	2.1	7.0	0.5	70.0	4.4	13.3	58.3	23.5	13.24	1779.5	13.4
3	0.13	2.3	2.1	7.0	0.5	107.0	17.3	13.3	229.7	12.1	26.4	7578.4	13.4
4	0.15	2.6	2.2	2.8	0.1	23.2	3.2	5.0	16.0	0.7	0.19	6.589	0.6
5	0.15	2.6	2.2	2.8	0.6	79.5	15.0	5.0	75.0	38.4	2.85	38.563	0.6
6	0.17	3.5	2.8	7.0	0.2	25.0	1.0	13.3	13.3	5.3	1.192	226.75	13.6
7	0.17	3.3	2.8	7.0	0.4	29.0	4.9	13.3	65.7	15.7	0.54	202.37	13.6
8	0.17	3.3	2.8	7.0	0.5	32.0	6.9	13.3	91.9	19.3	2.41	751.64	13.6
9	0.17	3.5	2.8	7.0	0.5	60.0	4.0	13.3	52.7	13.8	13.24	1631	13.6
10	0.17	3.5	2.8	7.0	0.5	93.0	18.2	13.3	241.8	24.2	26.4	8572.2	13.6
11	0.17	3.3	2.8	7.0	0.8	103.0	24.3	13.3	323.1	171.0	7.6	3000.2	13.6
12	0.18	4.0	3.2	2.8	0.1	25.5	4.7	5.3	25.1	3.3	0.2	5.09	0.4
13	0.18	4.0	3.2	2.8	0.6	45.1	9.6	5.3	51.0	8.3	3.03	31.093	0.4
14	0.18	4.0	3.2	2.8	0.9	67.2	21.1	5.3	111.8	73.1	6.5	52.44	0.4
15	0.20	17.0	7.0	5.4	0.1	3.8	2.8	11.6	32.6	3.7	0.118	55.564	10.7
16	0.20	17.0	7.0	5.4	0.2	10.3	9.3	11.6	107.0	8.9	0.571	246.54	10.7
17	0.20	17.0	7.0	5.4	0.5	26.5	21.8	11.6	252.0	12.3	1.81	1281.9	10.7
18	0.24	11.5	10.0	2.8	0.1	13.2	5.2	5.3	27.3	3.7	0.158	5.339	0.4
19	0.24	11.5	10.0	2.8	0.6	52.1	21.0	5.3	111.3	61.5	3.39	60.251	0.4
20	0.24	11.5	10.0	2.8	0.9	53.2	37.2	5.3	197.2	142.0	7.95	88.384	0.4
21	0.24	7.2	7.1	2.8	0.1	13.7	4.2	5.0	21.1	4.6	0.158	6.425	0.6
22	0.24	7.2	7.1	2.8	0.6	70.8	20.9	5.0	104.5	74.5	3.39	62.721	0.6
23	0.24	7.2	7.1	2.8	0.9	86.8	42.0	5.0	210.0	189.5	7.95	100.22	0.6
24	0.30	31.0	11.0	7.1	0.1	2.8	1.1	10.9	11.6	1.0	0.118	20.99	11.5
25	0.30	31.0	11.0	7.1	0.2	6.4	4.1	10.9	44.4	8.6	0.571	117.79	11.5
26	0.30	31.0	11.0	7.1	0.5	17.8	8.8	10.9	96.2	9.8	1.81	574.95	11.5
27	0.34	7.3	5.2	11.0	0.2	21.0	1.3	13.2	17.2	5.3	1.192	652.65	14.4
28	0.34	6.9	5.2	11.0	0.4	27.0	3.9	13.2	51.5	3.2	0.54	353.29	14.4
29	0.34	6.9	5.2	11.0	0.5	11.0	3.5	13.2	45.5	14.4	2.41	1274.5	14.4
30	0.34	7.3	5.2	11.0	0.5	35.0	4.2	13.2	55.0	13.7	13.24	2700.4	14.4
31	0.34	7.3	5.2	11.0	0.5	75.0	18.2	13.2	240.0	48.0	26.4	9187.1	14.4
32	0.34	6.9	5.2	11.0	0.8	58.0	27.1	13.2	358.2	94.2	7.6	3990.1	14.4

Note:

1) Rocking coefficient
2) Static factor of safety
3) Critical contact area ratio
4) Width of the foundation in the direction of foundation rocking
5) Maximum base acceleration
6) Total settlement of the foundation at the base center
7) Maximum rotation of the structure during foundation rocking
8) Height of structure to the center of gravity
9) Maximum tilt of the structure during foundation rocking
10) Permeant tilt of the structure at the end
11) Arias intensity
12) Dissipated energy at the foundation soil
13) V (m x g) is the total weight of the structure

References by # as follows,
Anastasopoulos et al. (2013): 7, 8, 11, 28, 29, 32
Drosos et al. (2012): 1-3, 6, 9, 10, 27, 30, 31
Gajan and Kutter (2008): 4, 5, 12-14, 18-23
Ugalde et al. (2007): 15-17, 24-26